Journal of Medicinal Chemistry

ARTICLE

pubs.acs.org/jmc

Organometallic Ruthenium(II) Arene Compounds with Antiangiogenic Activity

Patrycja Nowak-Sliwinska,[*,†,§,∥] Judy R. van Beijnum,[§,∥] Angela Casini,[*,‡] Alexey A. Nazarov,[‡] Georges Wagnières,[‡] Hubert van den Bergh,[†] Paul J. Dyson,[‡] and Arjan W. Griffioen[§]

[†]Institute of Bio-Engineering, Swiss Federal Institute of Technology (EPFL), Lausanne, Switzerland

[‡]Institute of Chemical Sciences and Engineering, Swiss Federal Institute of Technology (EPFL), Lausanne, Switzerland

[§]Angiogenesis Laboratory, Department of Medical Oncology, VU University Medical Center, Amsterdam, The Netherlands

ABSTRACT: The antimetastatic ruthenium(II) compounds [Ru(η^6-*p*-cymene)Cl_2(PTA)] (PTA = 1,3,5-triaza-7-phosphaadamantane) (RAPTA-C) and [Ru(η^6-toluene)Cl_2(PTA)] (RAPTA-T), as well as their analogues [Ru(η^6-*p*-cymene)Cl_2(DAPTA)] (DAPTA = (3,7-diacetyl-1,3,7-triaza-5-phosphabicyclo[3.3.1]nonane)) (DAPTA-C) and [Ru(η^6-toluene)Cl_2(DAPTA)] (DAPTA-T), respectively, were tested in in vitro bioassays for endothelial cell function. All compounds showed low toxicity profiles and similar dose-dependent antiproliferative effects in endothelial cells at ≥100 μg/mL (~200 μM). EC migration, measured 6 h after drug exposure, was also efficiently inhibited (ED_{50} of ~300 μg/mL, ~500 μM, for all compounds). Since no cytostatic effect was noted, the inhibition of proliferation was considered mainly to consist of antiangiogenic activity. RAPTA-T and DAPTA-C were also tested in vivo in the chicken chorioallantoic membrane (CAM) assay and found to inhibit CAM development. Importantly, effective prevention of revascularization of the CAM after vaso-occlusive photodynamic therapy was observed. The reported ruthenium complexes show promising antimetastatic activity involving inhibition of angiogenesis and therefore are attractive agents for development of anticancer therapies based on combination of chemo- and angiostatic treatments.

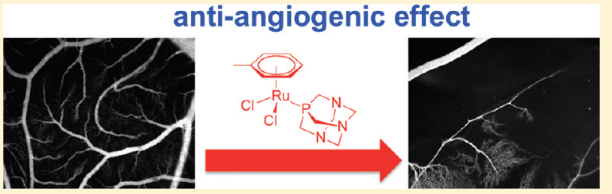

INTRODUCTION

Research on drugs based on ruthenium compounds is a fast developing field in medicinal chemistry/medicine, especially in relation to development of chemotherapeutics presenting minimal side effects and immunity to acquisition of drug resistance. Compared to other metal based drugs such as the platinum containing compounds cisplatin, carboplatin, and oxaliplatin,[1] ruthenium complexes appear to be promising.[2,3] Recently, two Ru(III) compounds, namely, KP1019 (indazolium *trans*-[tetrachlorobis(1*H*-indazole)ruthenate(III)]),[4] and NAMI-A (imidazolium *trans*-[tetrachloro(dimethylsulfoxide)(1*H*-imidazole)-ruthenate(III)]),[5] entered phase II clinical trials as anticancer compounds.

The specific mechanism of action of Ru(III) complexes is still not fully understood. The initial mechanistic hypothesis for these compounds was based on the so-called "activation by reduction" mechanism, according to which the Ru(III) complexes act as prodrugs that can be reduced to Ru(II) active species in the hypoxic (therefore reducing) environment of cancer cells.[6] Following the assumption that Ru(II) may be an important component of the final active drug, Ru(II) complexes have been synthesized and investigated for their antiproliferative properties.[7−9]

Interestingly, the bifunctional complexes of the general structural composition [Ru(η^6-arene)X_2(PTA)] (PTA = 1,3,5-triaza-7-phosphaadamantane) (RAPTA) showed antimetastatic properties and generally low toxicity comparable to those observed for NAMI-A.[8] For example, [Ru(η^6-*p*-cymene)Cl_2(PTA)] (RAPTA-C, Figure 1) has been shown to reduce the growth of lung metastases in CBA mice bearing the MCa breast carcinoma. This activity was observed in the absence of a corresponding activity at the site of primary tumor. In addition, RAPTA-C was also found to inhibit cell proliferation in vitro by arrest of cells in G2/M phase of cell cycle and induction of apoptosis, as observed in Ehrlich ascites carcinoma cells.[10]

Since the above-mentioned biological events and mechanisms of cell proliferation and invasion are involved in the processes of both metastases formation and angiogenesis,[11] we hypothesized that organometallic ruthenium(II) antimetastatic drugs may have antiangiogenic activity, as previously shown for NAMI-A.[12]

In general, RAPTA compounds seem to work via molecular targets other than DNA, implying a biochemical mode of action profoundly different from that of classical platinum anticancer drugs,[13] and it is likely that the mechanism of action of the RAPTA complexes may involve interactions with critical intracellular or extracellular proteins. For example, RAPTA compounds inhibit specific cysteine proteases involved in both cancer development and angiogenesis.[14]

Within this frame, the aim of the present study was to evaluate the angiostatic effects of RAPTA complexes in a series of in vitro bioassays. Therefore, RAPTA-C and RAPTA-T as well as two new other ruthenium compounds bearing the DAPTA ligand (3,7-diacetyl-1,3,7-triaza-5-phosphabicyclo[3.3.1]nonane), namely,

Received: February 23, 2011
Published: May 02, 2011

[Ru(η^6-*p*-cymene)Cl_2(DAPTA)] (DAPTA-C) and [Ru(η^6-toluene)Cl_2(DAPTA)] (DAPTA-T) (Figure 1), were characterized for their effect on angiogenesis of endothelial cells (EC). Afterward, we used the chicken embryo chorioallantoic membrane (CAM) model to study the rate and efficacy of angiogenesis inhibition of these compounds in vivo. Next to their effects on the natural in ovo CAM development, the influence of the ruthenium(II) compounds was evaluated in the CAM model by monitoring their influence on the regrowth of blood vessels after application of angio-occlusive photodynamic therapy. Research on the effect of photodynamic therapy (PDT) on the vasculature demonstrated that this treatment results in the induction of angiogenesis, which is the major rationale for combining PDT with antiangiogenesis therapy. Therefore, the ruthenium complexes, which have antiangiogenic properties, were applied after the PDT treatment. The results demonstrate that ruthenium compounds possess an intrinsic angiostatic activity, which makes these compounds attractive for further clinical development.

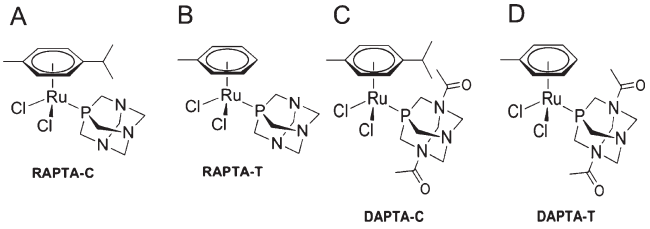

Figure 1. Ruthenium-based complexes used in this study: (A) RAPTA-C [Ru(η^6-*p*-cymene)Cl_2(PTA)], (B) RAPTA-T [Ru(η^6-toluene)Cl_2(PTA)], (C) DAPTA-C [Ru(η^6-*p*-cymene)Cl_2(DAPTA)], (D) DAPTA-T [Ru(η^6-toluene)Cl_2(DAPTA)], where PTA = 1,3,5-triaza-7-phosphatricyclo[3.3.1.1]decane (PTA) and DAPTA = 3,7-diacetyl-1,3,7-triaza-5-phosphabicyclo[3.3.1]nonane.

RESULTS

Ruthenium Compounds Inhibit Endothelial Cell Growth in Vitro. A series of ruthenium compounds, named RAPTA-C, RAPTA-T, DAPTA-C, and DAPTA-T (Figure 1A–D, respectively), were screened for their ability to inhibit cell growth in a series of EC growth assays. All compounds inhibited the viability of both primary (HUVEC) and immortalized (ECRF24) EC after 72 h of incubation, with ED_{50} of 300–500 μg/mL (~500–1000 μM) (see Figure 2A and Figure 2B). To evaluate whether ECs have a higher sensitivity to these compounds than cancer cells, the human colorectal tumor cell line LS174T was also

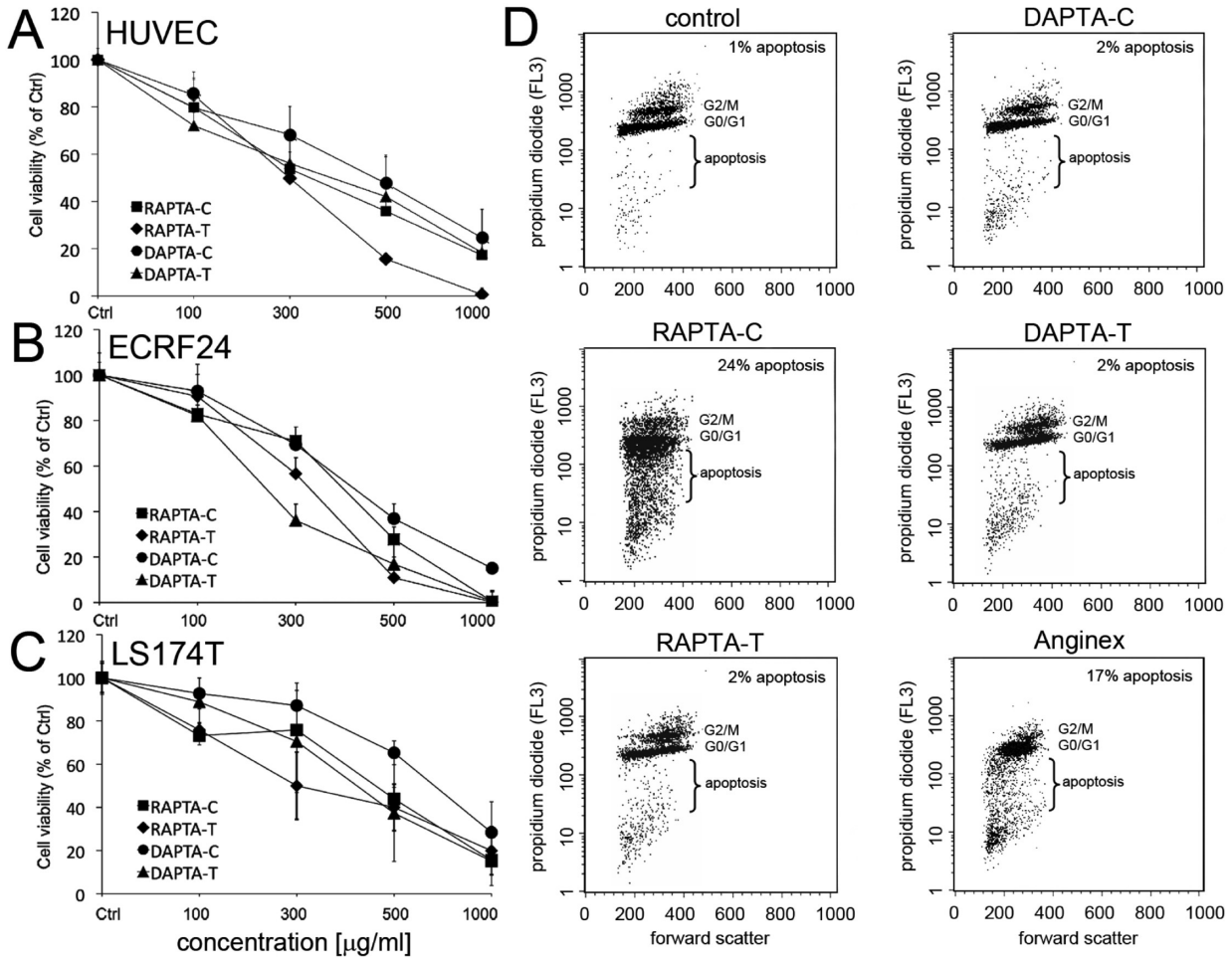

Figure 2. Effect of the Ru(II) arene complexes on cell proliferation and apoptosis. Effect of the RAPTA and DAPTA compounds on the proliferation of human umbilical vein endothelial cells (HUVEC) (A), the immortalized EC line ECRF24 (B), and human colon carcinoma cells (LS174T) (C). (D) Flow cytometrical analysis of the DNA content after fixation of the cells in 70% ethanol, a DNA extraction step, and staining with PI. Ruthenium complexes were tested at 300 μg/mL, and the results were compared with the addition of solvent alone. Anginex (10 μM) was used as the positive control.[15]

dx.doi.org/10.1021/jm2002074 |*J. Med. Chem.* 2011, 54, 3895–3902

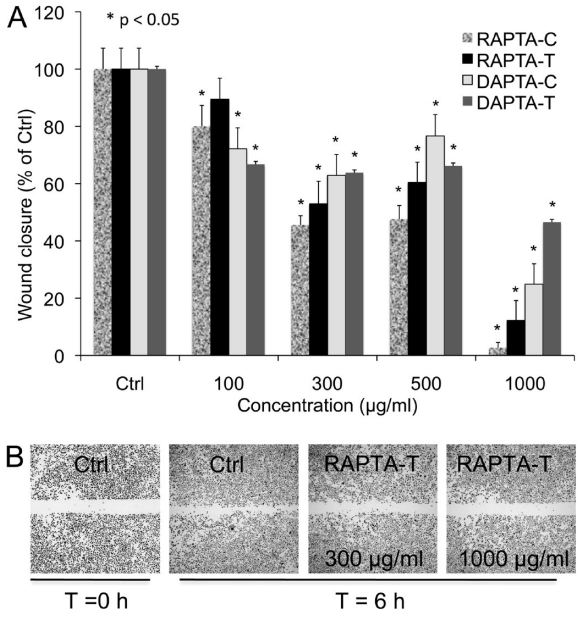

Figure 3. Effect of the Ru(II) arene complexes in the endothelial cell migration assay. (A) Concentration-dependent wound closure in ECRF24 cultures after 6 h of incubation with RAPTA and DAPTA complexes. $P < 0.05$ was considered to be statistically significant. (B) Typical images of the wound at the beginning of the experiment (culture medium as a control) and after 6 h of incubation with RAPTA-T shown at 300 and at 1000 μg/mL.

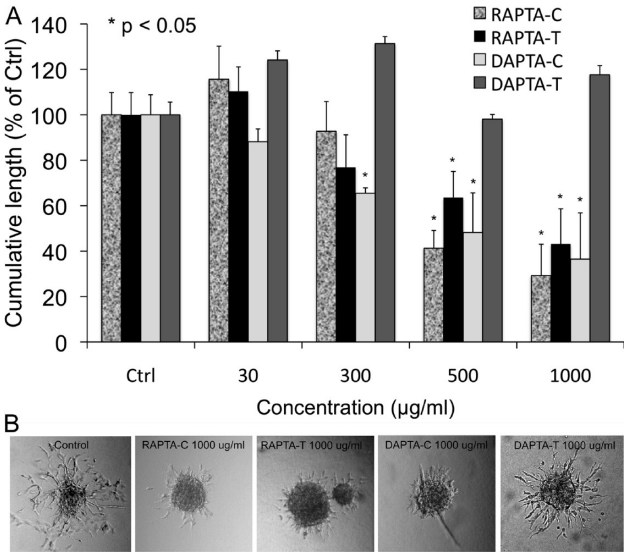

Figure 4. Effect of the ruthenium(II) complexes on endothelial sprout formation in vitro. (A) Concentration-dependent inhibition of endothelial sprout length, expressed as the percentage of the control, of HUVEC cells after 16 h of incubation with the RAPTA and DAPTA compounds. $P < 0.05$ was considered statistically significant. (B) Typical images of sprouting spheroids 16 h after incubation in the culture medium (control) or with the four ruthenium complexes at 1000 μg/mL.

studied (see Figure 2C). Similar ED_{50} values as those for the EC were observed in LS174T cells for the RAPTA compounds and for DAPTA-T, while a slightly less pronounced effect was noted for DAPTA-C. For all compounds a maximal effect close to 100% inhibition of proliferation was observed at 1 mg/mL (~2 mM).

In order to investigate whether the compounds induce apoptosis, DNA profiles of treated cells were analyzed by flow cytometry after staining with PI (see Figure 2D). Apoptosis induction, as reflected by DNA fragmentation in the cells, was tested for RAPTA and DAPTA complexes, as well as for the positive control anginex (10 μM), an angiogenesis inhibitor known to act via an apoptosis-inducing mechanism.[15] Apoptosis was observed only for RAPTA-C (24% of gated cells in apoptosis at 300 μg/mL). With RAPTA-T and DAPTA compounds' apoptosis (2% of cells) did not significantly exceed the levels of the cells that received only 0.9% NaCl (1% cells). In the positive control, anginex, 17% of the gated cells underwent apoptosis (Figure 2D).

Ruthenium Complexes Inhibit Endothelial Cell Migration and Sprout Formation in Vitro. As a second indication of activity of the ruthenium complexes on EC function, migration assays were performed using ECRF24 cells. As shown in Figure 3, the ruthenium complexes dose-dependently diminished the motility of EC at ≥100 μg/mL (~200 μM), and the ED_{50} values were approximately 300 μg/mL (~500 μM) for all compounds. Migration was >90% inhibited at 1 mg/mL (~2 mM) (Figure 3A) for RAPTA complexes, while DAPTA compounds were clearly less active. Migration of cells was measured 6 h after exposure to the compounds, and since cell proliferation, evaluated in parallel, was not affected after this short time period, the inhibition of migration is likely to result from an antiangiogenic activity.

Figure 3B shows the scratch wounds in ECRF24 cultures before and after 6 h of incubation with RAPTA-T. At this time point, the wound in the control wells was almost fully repopulated with migrated cells, while migration was inhibited gradually with increasing concentrations of the compounds (300 and 1000 μg/mL are presented). Primary ECs, i.e., HUVECs, were observed to behave similarly (data not shown).

To assess whether the ruthenium complexes can inhibit in vitro angiogenesis, we tested the compounds in an EC sprouting (bFGF-driven) assay using primary ECs (HUVEC) that display a better capacity to sprout. The obtained results show that the RAPTA compounds and DAPTA-C inhibited endothelial sprout formation in a dose-dependent manner with an ED_{50} of ~500 μg/mL (~1 mM) (see Figure 4A), while DAPTA-T did not inhibit sprout formation at any of the tested concentrations. Representative images are reported in Figure 4B showing endothelial sprouting 16 h after bFGF exposure in control conditions and after treatment with 1 mg/mL RAPTA-C, RAPTA-T, DAPTA-C, DAPTA-T.

Hampered Vessel Formation in the Developmental CAM. The antiangiogenic activity of the ruthenium complexes was investigated in vivo using the chicken embryo chorioallantoic membrane (CAM) assay. On the basis of the results described above, in vivo studies were continued with only RAPTA-T and DAPTA-C complexes.

The ruthenium complexes were topically applied (20 μL) at concentrations from 32 to 280 (μg/embryo)/day as homogeneous solutions in 0.9% NaCl. All embryos survived the full execution time of the experiments, which was 48 h, suggesting a good biocompatibility of the tested agents under the applied conditions. Figure 5 shows a typical image for the RAPTA-T and DAPTA-C complexes, and Table 1 reports the values of the three relevant descriptor values. In control-treated embryos (0.9% NaCl, Figure 5A), the capillary plexus was well developed, and

dx.doi.org/10.1021/jm2002074 |J. Med. Chem. 2011, 54, 3895–3902

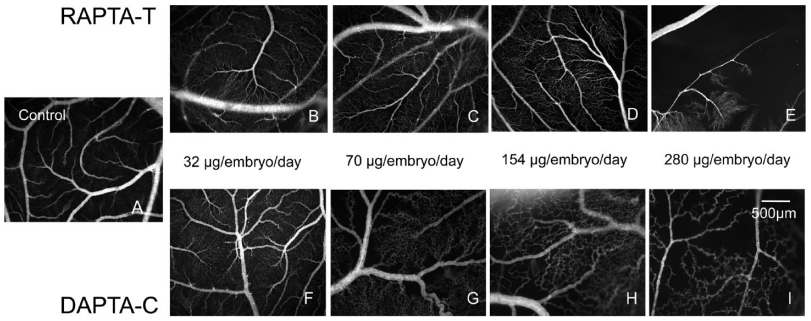

Figure 5. Angiographic images of the developmental CAM (EDD 9) treated with Ru(II) arene complexes. The vasculature is visualized by FITC-dextran fluorescence angiography (25 mg/kg, 20 kDa, λ_{ex} = 470 nm, λ_{em} = 520 nm). (A) Untreated CAM showing small vessels and capillary network. (B−E) Angiographies of CAMs treated with indicated RAPTA-T concentrations. (F−I) Angiographies of CAMs treated with indicated DAPTA-C concentrations. RAPTA-T and DAPTA-C were administrated at the following concentrations: 32 (μg/embryo)/day (image B and F), 70 (μg/embryo)/day (images C and G), 154 (μg/embryo)/day (images D and H), and 280 (μg/embryo)/day (images E and I).

Table 1. Values of Quantitative Descriptors for Control (0.9% NaCl) and DAPTA-C and RAPTA-T (32−280 (μg/Embryo)/Day) Treated CAMs[a]

			(μg/embryo)/day			
descriptor	control		32	70	154	280
branching points/mm^2	2313 ± 129	RAPTA-T	1450 ± 290	950 ± 210	520 ± 130	80 ± 30
		DAPTA-C	1750 ± 230	1320 ± 245	840 ± 123	290 ± 26
mean area of the vessel network meshes (10^2 μm^2)	4.2 ± 0.4	RAPTA-T	6.5 ± 2.5	16 ± 3.7	45 ± 8.0	na
		DAPTA-C	7.3 ± 1.3	9.5 ± 2.1	13 ± 2.1	41 ± 5.9
mean of the third quartile of mesh area histogram (10^2 μm^2)	6.2 ± 1.2	RAPTA-T	7.2 ± 1.9	32 ± 5.5	45 ± 8.1	na
		DAPTA-C	7.5 ± 2.1	20 ± 3.7	23 ± 3.3	97 ± 20

[a] Error bars represent standard error of mean. For RAPTA-T at 280 (μg/embryo)/day the quantification was not applied (na).

a homogeneous vascularization was observed. Following topical administration of the ruthenium complexes on the CAM, neovascularization was dose-dependently suppressed (see Figure 5B−E for RAPTA-T and Figure 5F−I for DAPTA-C). Avascular zones close to the vessel trunk appeared. The number and size of the avascular zones were comparable at 32 (μg/embryo)/day for RAPTA-T (Figure 5B) and DAPTA-C (Figure 5F), reducing number of branching points/mm^2 ± standard error of the mean from 2313 ± 129 (control) to 1450 ± 290 and 1750 ± 230 per 10^2 μm^2 for RAPTA-T and DAPTA-C, respectively (Figure 5).

Progressive disorganization of the capillary plexus was observed at 70 (μg/embryo)/day (Figure 5C and Figure 5G for RAPTA-T and DAPTA-C, respectively). The number of branching points/mm^2 decreased from 2313 ± 129 (control) to 950 ± 210 and 1320 ± 245 per 10^2 μm^2 for RAPTA-T and DAPTA-C, respectively. The mean of the third quartile of the mesh area histogram increased more than 2-fold, from 6.2 ± 1.2 for the control to 16.0 ± 3.7 for the RAPTA-T-treated CAMs (70 (μg/embryo)/day).

A more pronounced difference between the RAPTA-T and DAPTA-C efficacy was observed at a higher concentration (154 (μg/embryo)/day). The number of branching points/mm^2 was reduced by 78% (520 ± 130) by RAPTA-T and by 63% (840 ± 123) by DAPTA-C compared to the controls. The pronounced alteration of ruthenium complex treated CAMs, with respect to the control, was also evidenced by the values of the other two descriptors (see Table 1).

Administration of RAPTA-T at the highest concentration of 280 (μg/embryo)/day destroyed the capillary bed completely in the entire treated area and caused vasoconstriction of existing larger vessels (see Figure 5E). For this reason the quantification of vascular effects after the administration of RAPTA-T at 280 (μg/embryo)/day was not applicable. Administration of the same concentration of DAPTA-C (see Figure 5I), caused a less pronounced but still observable effect. The number of branching points/mm^2 decreased to 290 ± 26 per 10^2 μm^2. The mean area of the vessel network meshes (per 10^2 μm^2) was 10-fold bigger than for the control, and the mean of the third quartile of the mesh area histogram increased to 97 ± 20 (10^2 μm^2).

Effective Inhibition of Postphotodynamic Therapy Angiogenesis. Subsequently, the ruthenium complexes were tested in an in vivo model of photodynamic therapy (PDT) induced angiogenesis. This model allowed the evolution of the vascular network to be monitored, especially in terms of vascular occlusion and regrowth, during 2 days following treatment as described previously.[16,17] Research on the effect of PDT on the vasculature demonstrated that this treatment results in the induction of angiogenesis, which is the major rationale for combining PDT with antiangiogenesis therapy. Therefore, the ruthenium complexes, as shown above to have antiangiogenic properties, were applied after the PDT treatment. Twenty-four hours after angio-occlusive PDT (see Figure 6A) new vessels are formed, replacing the original occluded capillary plexus, a process that is completed for the treated area within 48 h, as shown in Figure 6B. As we previously described, the architecture of these newly formed vessels is changed to a more tortuous and less organized structure when compared to the original capillary plexus.[17]

dx.doi.org/10.1021/jm2002074 |J. Med. Chem. 2011, 54, 3895–3902

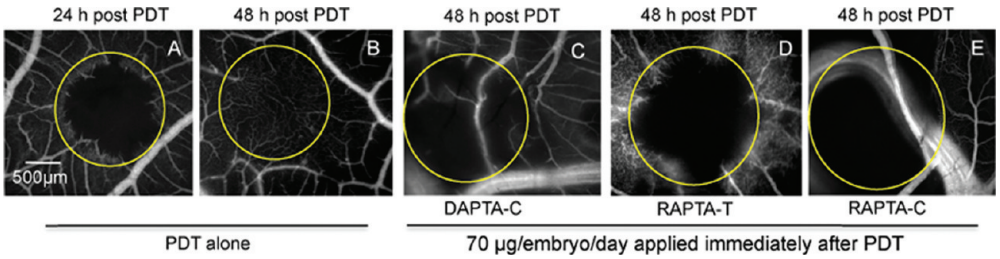

Figure 6. Inhibition of angio-occlusive photodynamic therapy (PDT) induced angiogenesis. Images visualized by FITC-dextran fluorescence angiography (25 mg/kg, 20 kDa, λ_{ex} = 470 nm, λ_{em} = 520 nm) of the CAM (EDD 13) after treatment with PDT alone (A and B) or in combination with immediate post-PDT topical application of the ruthenium complexes. Verteporfin-based PDT (0.20 mg/kg, iv, embryo weight, λ_{ex} = 420 nm) was performed at a light dose of 20 J/cm^2 and an irradiance of 50 mW/cm^2 and drug light interval of 1 min. (A) Full angio-occlusion in the PDT area 24 h after PDT. (B) Natural vascular regrowth 48 h after PDT within the treated area. Images C−E were taken 48 h after PDT followed by the topical administration of 70 (μg/embryo)/day of DAPTA-C (C), RAPTA-T (D), and RAPTA-C (E).

Topical application of ruthenium compounds immediately after PDT inhibited the vascular regrowth in the PDT-treated area. This inhibition was more efficient with increasing drug concentrations. Topical application of DAPTA-C at 32 (μg/embryo)/day already resulted in only partial vascular regrowth, with the central part of the PDT-treated area still remaining avascular after 48 h of incubation after PDT (data not shown). Topically administrated DAPTA-C at 70 (μg/embryo)/day, a concentration that produces only a moderate effect in CAM development (see Figure 5), significantly inhibited post-PDT angiogenesis but did not influence the vessel reperfusion process (see Figure 5C). RAPTA-T administered at the same concentration resulted in massive inhibition of angiogenesis and prevention of reperfusion of pre-existing vessels (see Figure 6D). The strongest effect was observed for RAPTA-C administered at the same concentration (see Figure 6E).

DISCUSSION AND CONCLUSIONS

Ruthenium-based compounds have been recently described as potential anticancer drugs,[5,18−20] and it was shown that certain ruthenium complexes manifest higher efficiency against metastases than primary tumors.[21] These properties, also shared by the RAPTA compounds developed by some of us, are attractive for the development of new classes of antitumor drugs. In this study we investigated whether the promising anticancer activities of two RAPTA compounds and of their respective DAPTA derivatives are partly based on an intrinsic antiangiogenic activity, as it has previously been demonstrated for the taxanes,[22] and for the antimetastatic Ru(III) compound NAMI-A. It was found that RAPTA and DAPTA complexes can inhibit a number of in vitro EC functions essential in angiogenesis, such as proliferation, migration, and tube formation. Using assays for these EC functions, we endeavored to search for activity at concentrations or time periods that do not display toxic or antiproliferative effects, since this would indicate an intrinsic angiostatic activity.

The presented results showed that both RAPTA and DAPTA complexes display inhibitory effects on the metabolism and proliferation of freshly isolated EC and of an immortalized EC line, namely, HUVEC and ECRF24, respectively. For RAPTA-C, inhibition of proliferation involved induction of apoptosis, while for the other compounds apoptosis was not observed. Interestingly, it was found that cells of endothelial origin were slightly more sensitive than tumor cells, suggesting that the cytostatic compounds have intrinsic angiostatic properties, as described previously for chemotherapeutic compounds such as paclitaxel.[22] Although this higher sensitivity of ECs is noteworthy, it can be argued that all antiproliferative (chemotherapeutic) agents can have antiangiogenic activity because of the location of the endothelium, being the first to be in contact with the blood.

Moreover, the compounds were tested for their effects on migration of ECs, and it was found that significant inhibition of migration ($p < 0.05$) was observed already at 100 μg/mL (~200 μM) after 6 h of exposure. Since this concentration does not affect endothelial cell proliferation and certainly not after an exposure time of only 6 h, these compounds harbor an angiostatic activity. It is surprising that sprouting of EC seemed to be less inhibited by RAPTA complexes and DAPTA-C compounds (DAPTA-T was completely ineffective), which reveal activity only at >300 μg/mL following 16 h of drug treatment. From this assay it also appears that the compounds affect the sprout length.

The results out of the in vivo chicken chorioallantoic membrane model (CAM) assays further confirm the inhibition of angiogenesis by ruthenium complexes. In fact, in the developmental CAM model (embryo development days (EDDs) 7−9)[16] clear inhibition of vessel formation is shown resulting in large avascular zones in the CAM, suggesting that antitumor activity of these compounds involves, to some extent, inhibition of angiogenesis.

It is worth noting that previous studies on the ruthenium(III) complex NAMI-A on similar in vitro and in vivo angiogenesis models showed comparable properties with those observed for our RAPTA/DAPTA compounds.[12] Interestingly, in the latter study it was shown that the relatively high concentrations of NAMI-A (in the range 100−300 μM) active in vitro on EC functions, and efficacy in vivo in the CAM model, are easily reached from the beginning of the schedule of antimetastasis treatment in CBA mice bearing the MCa mammary carcinoma.[8] Since RAPTA compounds were also reported to have similar behavior as NAMI-A in reducing the growth of lung metastases in the same mouse model[23] and that the percentages of ruthenium recovered in the body for RAPTA complexes can be compared to the retention of the antimetastatic NAMI-A compound, we believe that the tested high concentrations of complexes in our antiangiogenic models can be reached also in vivo.

Finally, screening of the compounds in a therapeutic model was also performed by measuring the vascular regrowth after exposure of the mature CAM to angio-occlusive PDT combined with the subsequent topical administration of the ruthenium complexes (see Experimental Section for details). In this assay, a dose of 70 (μg/embryo)/day already blocked close to 100% of vascular regrowth in the PDT area. This result is of interest because the same dose induced readily visible but still only

dx.doi.org/10.1021/jm2002074 |J. Med. Chem. 2011, 54, 3895–3902

moderate inhibition of the developmental CAM. Apparently, it takes more effort to inhibit developmental angiogenesis than angiogenesis induced by a sudden challenge such as exposure to PDT. This observation strongly suggest that the combined use of PDT and ruthenium complexes may prevent the recurrence of conditions treated by PDT, as it is the case for age-related macular degeneration.[24]

The herein reported results show that both the RAPTA and DAPTA compounds, with RAPTA-C as the most promising compound, inhibit angiogenesis. Indeed, further studies need to be developed to highlight the molecular mechanisms through which the observed effects are elicited, although the interactions of the ruthenium compounds with proteins/enzymes crucial to both the metastatic and angiogenic processes should be considered, including proteases, kinases, and vascular growth factors.[25] In this context, apart from the above-mentioned inhibition of cysteine proteases,[14] preliminary results of in vitro enzyme inhibition of 100 human kinases indicate that RAPTA compounds are selective inhibitors of the fibroblast growth factor receptor (FGF-R1) and of the vascular endothelial growth factor receptor (VEGFR) involved in tumor growth and angiogenesis.[25,26]

From a mechanistic point of view it must be noted that RAPTA/DAPTA complexes can behave as prodrugs undergoing hydrolysis processes (e.g., of the chloride ligands) to be able to interact with biomolecules[7,27] However, especially in the extracellular environment where the concentration of chloride is relatively high (~100 mM) direct reaction between RAPTA/DAPTA complexes and a protein target (i.e., prior aquation) is possible, although reactivity is considerably slower.[28]

In any case, the possible combination of cytostatic and antiangiogenic activity in a stable and small molecule drug is very attractive. Since it has been demonstrated that VEGF targeting with bevacizumab (humanized monoclonal antibody) or small molecule tyrosine kinase inhibitors may induce metastasis, the previous demonstration of RAPTA-C to be antimetastatic is therefore very relevant. On the basis of these considerations, ruthenium-based compounds are attractive agents for development of future anticancer therapies relying on the combination of chemo- and angiostatic therapy.

EXPERIMENTAL SECTION

Reagents and Cells. All reactions were carried out in dry solvents under an inert atmosphere. Chemicals were obtained from commercial suppliers and used as received. The purity of the Ru compounds was confirmed by elemental analysis, and all of them showed purity greater than 98%. ^{1}H and ^{31}P NMR spectra[29] were recorded at 25 °C on a Bruker Avance 400 FT NMR spectrometer (Bruker, Billerica, MA, U.S.).

Human umbilical vein endothelial cells (HUVEC) were isolated from fresh human umbilical cord veins and maintained in RPMI-1640 (Invitrogen, Carlsbad, CA, U.S.) supplemented with 10% human serum, 10% FCS, 1% glutamin (Invitrogen), 100 IU/mL penicillin (Sigma-Aldrich, St. Louis, MO, U.S.), and 100 μg/mL streptomycin (Sigma-Aldrich, St. Louis, MO, U.S.) as previously described.[30] The immortalized endothelial cell (EC) line ECRF24[31] was grown in the same medium. The human colon carcinoma cell line LS174T was grown in DMEM (Life Technologies, Carlsbad, CA, U.S.) supplemented with 10% FCS, glutamine, and antibiotics as mentioned above. All cells were cultured in a highly humidified atmosphere with 5% CO_2 at 37 °C.

Synthesis of the Ru(II) Arene Compounds. The dimers bis[dichlorido(η^6-*p*-cymene)ruthenium(II)][32] and bis[dichlorido(η^6-toluene)ruthenium(II)][33] were synthesized using literature procedures. The ligands 1,3,5-triaza-7-phosphatricyclo[3.3.1.1]decane (PTA) and 3,7-diacetyl-1,3,7-triaza-5-phosphabicyclo[3.3.1]nonane (DAPTA) were prepared as previously reported.[34,35] [Ru(η^6-*p*-cymene)Cl_2(PTA)] (RAPTA-C, Figure 1A), [Ru(η^6-toluene)Cl_2(PTA)] (RAPTA-T, Figure 1B), and [Ru(η^6-*p*-cymene)Cl_2DAPTA] (DAPTA-C, Figure 1C) were synthesized as described before.[8,36,37] DAPTA-T (see Figure 1D) [Ru(η^6-toluene)Cl_2(DAPTA)] is a new compound and was prepared as follows. A solution of DAPTA (0.92 g, 4 mmol) in 100 mL of MeOH was added to a solution of [$RuCl_2(\eta^6$-toluene)$_2$] (1.05 g, 2 mmol) in 100 mL of CH_2Cl_2. The reaction mixture was stirred for 10 h at room temperature. The resulting solution was then concentrated to ~20 mL, and 100 mL of diethyl ether was added, yielding a microcrystalline orange solid material that was washed with diethyl ether (3 × 20 mL) and dried under vacuum. Yield: 1.59 g (81%), mp > 230 (dec). Anal. Calcd for $RuC_{16}H_{24}N_3Cl_2O_2P$ (%): C 38.95, H 4.90, N 8.52. Found: C 38.77, H 4.92, N 8.63. NMR ^{31}P ($CDCl_3$): δ = −11.6 ppm. ^{1}H NMR ($CDCl_3$): δ = 2.12 (s, 6H, $COCH_3$), 2.30 (s, 3H, CH_3), 3.79 (d, 1H, *J* = 15.5 Hz, PCH_2N), 3.94−4.06 (m, 3H, PCH_2N), 4.38 (d, 1H, *J* = 15.2 Hz, NCH_2N), 4.59−4.67 (m, 2H, PCH_2N, NCH_2N), 5.00 (d, 1H, *J* = 14.0 Hz, NCH_2N), 5.28 (tr, 1H, *J* = 4.7 Hz, NCH_2P), 5.49 (m, 2H, C_6H_5), 5.59−5.72 (m, 3H, C_6H_5), 5.80 (d, 1H, *J* = 13.5 Hz, NCH_2N) ppm.

Proliferation Assay. ECs (5 × 10^3 cells/well) were seeded in gelatin-coated 96-well cell culture plates as described previously.[38] Briefly, 24 h after seeding, culture medium with or without ruthenium compounds was added and cells were grown for a further 72 h. Simultaneously, the same assay was performed for 6 h, which corresponds to the duration of the wound assay, in order to exclude the influence of cytotoxic effect from the migration process. Cell viability was assessed using the CellTiter-Glo luminescent cell viability assay (Promega, Madison, WI, U.S.). Alternatively, cells were counted using propidium iodide (PI) staining.[39] Briefly, cells were seeded and treated as above and subsequently washed with PBS and fixed in the 96-well plates with ice-cold 70% ethanol at −20 °C for 2−16 h. Cells were washed with PBS and incubated with PBS containing 10 μg/mL PI and 100 μg/mL RNase A (Fermentas International Inc.; Burlington, Canada), for 1 h at 37 °C. Plates were scanned in an Acumen eX3 cytometer (TTP LabTech Ltd., Royston, U.K.), and fluorescent objects were identified using Acumen eX3 cytometry software. Size parameters were set to exclude cell debris and duplexes, and cell numbers were obtained per well.

Propidium Iodide (PI) Staining. Apoptosis was measured by flow cytometric determination of subdiploid cells after DNA extraction and subsequent staining with PI as described before.[40] Briefly, cells were harvested and subsequently fixed in 70% ethanol at −20 °C. After 2 h the cells were resuspended in DNA extraction buffer (45 mM Na_2HPO_4, 2.5 mM citric acid, and 1% Triton X-100, pH 7.4) for 20 min at 37 °C. PI was added to a final concentration of 20 μg/mL and log scale red fluorescence was analyzed on a FACSCalibur (BD Biosciences, NJ, U.S.). Apoptosis was quantified as the percentage of subdiploid cells.

Wound Assay (Migration). The migration capability of ECs was measured using the wound assay.[41] In brief, HUVEC and ECRF24 cultures were grown to confluence in gelatin-coated wells. Cells were labeled with calcein AM (Molecular Probes, C3100MP, Carlsbad, CA, U.S.) for 15 min (1:2000, Molecular Probes), and "scratch wounds" (with an approximate width of 350 μm) were made in the monolayer by removing cells with a sterile scratch tool (Peira Scientific Instruments, Beerse, Belgium). Cultures were washed with PBS, and the medium was replaced by fresh medium containing 10 ng/mL bFGF (Tebu-Bio) and incubated with or without ruthenium compounds at the dose range 100−1000 μg/mL. Plates were scanned using an Acumen eX3 laser scanner cytometer (TTP LabTech Ltd., Royston, U.K.) to acquire images for computational analysis of scratch sizes using UGR Scratch Assay 6.2 software (DCI Labs, Peira Scientific Instruments).

Endothelial Cell Sprouting Assay. EC spheroids were created using the hanging drop method. ECs were suspended in medium containing 20% methocel (Sigma-Aldrich, St. Louis, MO, U.S.) at 4×10^4 cells/mL, and 25 μL drops (containing 1000 cells) were aliquoted on the inside of the lid of a Petri dish. The lid was subsequently inverted to create the hanging drops and placed over the PBS containing Petri dish. After 24 h the spheroids were harvested and embedded in a collagen gel (2 mg/mL) at 20 spheroids per well of a 96-well plate. After solidification of the gel, the medium containing the test compounds was added and cells were allowed to sprout into the collagen for 16 h.

Sprouting spheroids (8−10 per condition) were pictured directly under a microscope (Leica Microsystems GmbH, Wetzlar, Germany) under 10× magnification. Quantification of sprouting was performed using a semi-automatic macro written by Dr. Jean-Pierre Ballini and Dr. Patrycja Nowak-Sliwinska (Medical Photonics Group, Swiss Federal Institute of Technology (EPFL), Lausanne, Switzerland) based on the ImageJ platform. The macro asks the user to create a circular region of interest (ROI) in the image corresponding to the shape and the size of the spheroid. By manual clicking to the end point of each sprout (indicating the X and Y coordinates) on the original picture, this macro interactively measures the length, total sum of length, and the number of sprouts measured from the end point to the border of the previously created circular ROI. The results are given in pixels that can be further scaled to micrometers.

Developmental CAM and Quantification of the Angiogenic Response. In this assay the antiangiogenic efficacy of the ruthenium complexes was tested in the physiologically developing chicken embryo chorioallantoic membrane (CAM) model between embryo development days (EDDs) 7 and 9 as previously described in detail.[16] Briefly, ruthenium compounds were applied topically twice (each time 20 μL), at EDDs 7 and 8, at concentrations ranging from 10 to 280 (μg/embryo)/day. The control eggs twice received (each time 20 μL) 0.9% NaCl. At EDD 9, the CAMs were visualized in ovo by means of FITC-dextran (20 kDa, 25 mg/mL, Sigma-Aldrich) epi-fluorescence angiography and subsequently analyzed by the image-processing quantification method described previously.[16] Briefly, on the basis of FITC-dextran fluorescence angiography, the skeleton of the vascular network is built, and defined descriptors, i.e., branching points/mm^2, the mean area of the vessel network meshes (10^2 μm^2), and the mean of the third quartile of mesh area histogram ($10^2\mu$m^2), give information on the vascular architecture. Eight to 10 eggs were tested per condition.

Ruthenium(II) Arene Compounds in Combination with Visudyne Photodynamic Therapy on the CAM. Visudyne photodynamic therapy (PDT) was performed, as described elsewhere,[17,42,43] prior to topical administration of ruthenium compounds. Briefly, on EDD 11, a volume of 10 μL (0.20 mg of verteporfin/kg) of Visudyne (the liposomal formulation of verteporfin, Novartis Pharma, Inc., Hettlingen, Switzerland) was intravenously administered through a 33 gauge needle fitted to a 100 μL syringe (Hamilton, Reno, NV, U.S.) into the main vessel of the CAM. One minute after injection, the site with vessels of diameter between 5 and about 70 μm was irradiated with a light dose of 20 J/cm^2 (λ_{ex}= 420 ± 20 nm, Nikon, Japan) with irradiance of 50 mW/cm^2. Ruthenium compounds were deposited topically twice (immediately after PDT and 24 h after PDT) to the surface of the CAM in the form of liquid drops (each time 20 μL) at concentrations between 32 and 280 (μg/embryo)/day within a polyethylene ring (diameter 5 mm, wall thickness 0.5 mm, 1 mm height). Fluorescence angiograms of PDT areas were taken after 24 and 48 h by means of FITC-dextran (20 kDa, 25 mg/mL, Sigma-Aldrich) epi-fluorescence angiography with the same microscope. For detection of FITC, light was filtered for excitation at 470 ± 20 nm, and a long-pass emission filter was used for detection of the fluorescence (λ > 520 nm, Nikon, Japan). Fluorescence images were acquired with an F-view II 12-bit monochrome Peltier-cooled digital CCD camera driven with analySIS DOCU software from Soft Imaging System.

Statistical Analysis. Values are given as the mean ± SD. Data are represented as averages of independent experiments, performed in duplicate or triplicate. Statistical analyses were done using the Student's t test. $P < 0.05$ was considered statistically significant.

AUTHOR INFORMATION

Corresponding Author

*For P.N.-S.: phone, +41-21-6935169; fax, +41-21-6935110; e-mail, patrycja.nowak-sliwinska@epfl.ch. For A.C.: phone, +41-21-6939860; fax, +41-21-6939780; e-mail, angela.casini@epfl.ch.

Author Contributions

‖ These authors contributed equally to this study.

ACKNOWLEDGMENT

The authors are grateful for financial support from Dr. Julia Jacobi. The authors thank Dr. Jean-Pierre Ballini for expert technical advice, Saskia van der Velden and Maaike van Berkel for excellent technical assistance, and the Neuro-Oncology Research Group and CCA Stichting Avanti-STR for use of Acumen eX3. A.C. thanks the Swiss National Science Foundation (SNSF) (AMBIZIONE Project No. PZ00P2-121933/1 and Project No. 205320-130518/1), the Swiss Confederation (Action COST D39, Accord de Recherché, SER Project No. C09.0027) and COST D39, and EPFL for financial support. The authors thank Roxane Oberson for the synthesis of the PTA and DAPTA ligands.

ABBREVIATIONS USED

CAM, chicken chorioallantoic membrane; DAPTA, 3,7-diacetyl-1,3,7-triaza-5-phosphabicyclo[3.3.1]nonane; EC, endothelial cell; ECRF24, immortalized endothelial cell line; EDD, embryo development day; FGF-R1, fibroblast growth factor receptor; HUVEC, human umbilical vein endothelial cell; LS174T, human colon carcinoma cell line; PI, propidium iodide; PDT, photodynamic therapy; PTA, 1,3,5-triaza-7-phosphaadamantane; ROI, region of interest; VEGF, vascular endothelial growth factor; VEGFR, vascular endothelial growth factor receptor

REFERENCES

(1) Muggia, F. Platinum compounds 30 years after the introduction of cisplatin: implications for the treatment of ovarian cancer. *Gynecol. Oncol.* **2009**, *112*, 275–281.

(2) Gianferrara, T.; Bratsos, I.; Alessio, E. A categorization of metal anticancer compounds based on their mode of action. *Dalton Trans.* **2009**, 7588–7598.

(3) Hartinger, C. G.; Dyson, P. J. Bioorganometallic chemistry—from teaching paradigms to medicinal applications. *Chem. Soc. Rev.* **2009**, *38*, 391–401.

(4) Hartinger, C. G.; Jakupec, M. A.; Zorbas-Seifried, S.; Groessl, M.; Egger, A.; Berger, W.; Zorbas, H.; Dyson, P. J.; Keppler, B. K. KP1019, a new redox-active anticancer agent—preclinical development and results of a clinical phase I study in tumor patients. *Chem. Biodiversity* **2008**, *5*, 2140–2155.

(5) Sava, G.; Gagliardi, R.; Bergamo, A.; Alessio, E.; Mestroni, G. Treatment of metastases of solid mouse tumours by NAMI-A: comparison with cisplatin, cyclophosphamide and dacarbazine. *Anticancer Res.* **1999**, *19*, 969–972.

(6) Schluga, P.; Hartinger, C. G.; Egger, A.; Reisner, E.; Galanski, M.; Jakupec, M. A.; Keppler, B. K. Redox behavior of tumor-inhibiting ruthenium(III) complexes and effects of physiological reductants on their binding to GMP. *Dalton Trans.* **2006**, 1796–1802.

(7) Ang, W. H.; Casini, A.; Sava, G.; Dyson, P. J. Organometallic ruthenium-based antitumor compounds with novel modes of action. *J. Organomet. Chem.* **2011**, *696*, 989–998.
(8) Scolaro, C.; Bergamo, A.; Brescacin, L.; Delfino, R.; Cocchietto, M.; Laurenczy, G.; Geldbach, T. J.; Sava, G.; Dyson, P. J. In vitro and in vivo evaluation of ruthenium(II)-arene PTA complexes. *J. Med. Chem.* **2005**, *48*, 4161–4171.
(9) Hanif, M.; Nazarov, A. A.; Hartinger, C. G.; Kandioller, W.; Jakupec, M. A.; Arion, V. B.; Dyson, P. J.; Keppler, B. K. Osmium(II)- versus ruthenium(II)-arene carbohydrate-based anticancer compounds: similarities and differences. *Dalton Trans.* **2010**, *39*, 7345–7352.
(10) Chatterjee, S.; Kundu, S.; Bhattacharyya, A.; Hartinger, C. G.; Dyson, P. J. The ruthenium(II)-arene compound RAPTA-C induces apoptosis in EAC cells through mitochondrial and p53-JNK pathways. *J. Biol. Inorg. Chem.* **2008**, *13*, 1149–1155.
(11) Carmeliet, P.; Jain, R. K. Angiogenesis in cancer and other diseases. *Nature* **2000**, *407*, 249–257.
(12) Vacca, A.; Bruno, M.; Boccarelli, A.; Coluccia, M.; Ribatti, D.; Bergamo, A.; Garbisa, S.; Sartor, L.; Sava, G. Inhibition of endothelial cell functions and of angiogenesis by the metastasis inhibitor NAMI-A. *Br. J. Cancer* **2002**, *86*, 993–998.
(13) Dyson, P. J.; Sava, G. Metal-based antitumour drugs in the post genomic era. *Dalton Trans.* **2006**, 1929–1933.
(14) Casini, A.; Gabbiani, C.; Sorrentino, F.; Rigobello, M. P.; Bindoli, A.; Geldbach, T. J.; Marrone, A.; Re, N.; Hartinger, C. G.; Dyson, P. J.; Messori, L. Emerging protein targets for anticancer metallodrugs: inhibition of thioredoxin reductase and cathepsin B by antitumor ruthenium-(II)-arene compounds. *J. Med. Chem.* **2008**, *51*, 6773–6781.
(15) Griffioen, A. W.; van der Schaft, D. W.; Barendsz-Janson, A. F.; Cox, A.; Struijker Boudier, H. A.; Hillen, H. F.; Mayo, K. H. Anginex, a designed peptide that inhibits angiogenesis. *Biochem. J.* **2001**, *354*, 233–242.
(16) Nowak-Sliwinska, P.; Ballini, J. P.; Wagnieres, G.; van den Bergh, H. Processing of fluorescence angiograms for the quantification of vascular effects induced by anti-angiogenic agents in the CAM model. *Microvasc. Res.* **2010**, *79*, 21–28.
(17) Nowak-Sliwinska, P.; van Beijnum, J.; van Berkel, M.; van den Bergh, H.; Griffioen, A. Vascular regrowth following photodynamic therapy in the chicken embryo chorioallantoic membrane. *Angiogenesis* **2010**, *13*, 281–292.
(18) Bergamo, A.; Gagliardi, R.; Scarcia, V.; Furlani, A.; Alessio, E.; Mestroni, G.; Sava, G. In vitro cell cycle arrest, in vivo action on solid metastasizing tumors, and host toxicity of the antimetastatic drug NAMI-A and cisplatin. *J. Pharmacol. Exp. Ther.* **1999**, *289*, 559–564.
(19) Bergamo, A.; Masi, A.; Peacock, A. F.; Habtemariam, A.; Sadler, P. J.; Sava, G. In vivo tumour and metastasis reduction and in vitro effects on invasion assays of the ruthenium RM175 and osmium AFAP51 organometallics in the mammary cancer model. *J. Inorg. Biochem.* **2010**, *104*, 79–86.
(20) Antonarakis, E. S.; Emadi, A. Ruthenium-based chemotherapeutics: are they ready for prime time? *Cancer Chemother. Pharmacol.* **2010**, *66*, 1–9.
(21) Bergamo, A.; Masi, A.; Dyson, P. J.; Sava, G. Modulation of the metastatic progression of breast cancer with an organometallic ruthenium compound. *Int. J. Oncol.* **2008**, *33*, 1281–1289.
(22) Bocci, G.; Nicolaou, K. C.; Kerbel, R. S. Protracted low-dose effects on human endothelial cell proliferation and survival in vitro reveal a selective antiangiogenic window for various chemotherapeutic drugs. *Cancer Res.* **2002**, *62*, 6938–6943.
(23) Vacca, A.; Bruno, M.; Boccarelli, A.; Coluccia, M.; Ribatti, D.; Bergamo, A.; Garbisa, S.; Sartor, L.; Sava, G. Inhibition of endothelial cell functions and of angiogenesis by the metastasis inhibitor NAMI-A. *Br. J. Cancer* **2002**, *86*, 993–998.
(24) van den Bergh, H. Photodynamic therapy of age-related macular degeneration: history and principles. *Semin. Ophthalmol.* **2001**, *16*, 181–200.
(25) Cook, K. M.; Figg, W. D. Angiogenesis inhibitors: current strategies and future prospects. *Ca—Cancer J. Clin.* **2010**, *60*, 222–243.
(26) Korc, M.; Friesel, R. E. The role of fibroblast growth factors in tumor growth. *Curr. Cancer Drug Targets* **2009**, *9*, 639–651.
(27) Scolaro, C.; Hartinger, C. G.; Allardyce, C. S.; Keppler, B. K.; Dyson, P. J. Hydrolysis study of the bifunctional antitumour compound RAPTA-C, [Ru(eta(6)-*p*-cymene)Cl-2(pta). *J. Inorg. Biochem.* **2008**, *102*, 1743–1748.
(28) Groessl, M.; Hartinger, C. G.; Dyson, P. J.; Keppler, B. K. CZE-ICP-MS as a tool for studying the hydrolysis of ruthenium anticancer drug candidates and their reactivity towards the DNA model compound dGMP. *J. Inorg. Biochem.* **2008**, *102*, 1060–1065.
(29) Abels, C. Targeting of the vascular system of solid tumours by photodynamic therapy (PDT). *Photochem. Photobiol. Sci.* **2004**, *3*, 765–771.
(30) van Beijnum, J. R.; Dings, R. P.; van der Linden, E.; Zwaans, B. M.; Ramaekers, F. C.; Mayo, K. H.; Griffioen, A. W. Gene expression of tumor angiogenesis dissected: specific targeting of colon cancer angiogenic vasculature. *Blood* **2006**, *108*, 2339–2348.
(31) Fontijn, R.; Hop, C.; Brinkman, H. J.; Slater, R.; Westerveld, A.; van Mourik, J. A.; Pannekoek, H. Maintenance of vascular endothelial cell-specific properties after immortalization with an amphotrophic replication-deficient retrovirus containing human papilloma virus 16 E6/E7 DNA. *Exp. Cell Res.* **1995**, *216*, 199–207.
(32) Stahl, S.; Werner, H. A new family of (arene)osmium(0) and -osmium(II) complexes. *Organometallics* **1990**, *9*, 1876–1881.
(33) Bennett, M. A.; Smith, A. K. *J. Chem. Soc., Dalton Trans. (1972—1999)* **1974**, *2*, 233–241.
(34) Daigle, D. J. 1,3,5-Triaza-7-phosphatricyclo[3.3.1.13,7]decane and derivatives. *Inorg. Synth.* **1998**, *32*, 40–45.
(35) Darensbourg, D. J.; Ortiz, C. G.; Kamplain, J. W. A new water-soluble phosphine derived from 1,3,5-triaza-7-phosphaadamantane (PTA), 3,7-diacetyl-1,3,7-triaza-5-phosphabicyclo[3.3.1]nonane. Structural, bonding, and solubility properties. *Organometallics* **2004**, *23*, 1747–1754.
(36) Allardyce, C. S.; Dyson, P. J.; D.J., E.; S.L., H. [Ru(*η*6-*p*-cymene)Cl2(pta)] (pta = 1,3,5-triaza-7-phosphatricyclo-[3.3.1.1]decane): a water soluble compound that exhibits pH dependent DNA binding providing selectivity for diseased cells. *Chem. Commun.* **2001**, *15*, 1396–1397.
(37) Cadierno, V.; Francos, J.; Gimeno, J. Selective ruthenium-catalyzed hydration of nitriles to amides in pure aqueous medium under neutral conditions. *Chemistry* **2008**, *14*, 6601–6605.
(38) Brandwijk, R. J.; Nesmelova, I.; Dings, R. P.; Mayo, K. H.; Thijssen, V. L.; Griffioen, A. W. Cloning an artificial gene encoding angiostatic anginex: from designed peptide to functional recombinant protein. *Biochem. Biophys. Res. Commun.* **2005**, *333*, 1261–1268.
(39) Kittler, R.; Pelletier, L.; Heninger, A. K.; Slabicki, M.; Theis, M.; Miroslaw, L.; Poser, I.; Lawo, S.; Grabner, H.; Kozak, K.; Wagner, J.; Surendranath, V.; Richter, C.; Bowen, W.; Jackson, A. L.; Habermann, B.; Hyman, A. A.; Buchholz, F. Genome-scale RNAi profiling of cell division in human tissue culture cells. *Nat. Cell Biol.* **2007**, *9*, 1401–1412.
(40) van der Schaft, D. W.; Toebes, E. A.; Haseman, J. R.; Mayo, K. H.; Griffioen, A. W. Bactericidal/permeability-increasing protein (BPI) inhibits angiogenesis via induction of apoptosis in vascular endothelial cells. *Blood* **2000**, *96*, 176–181.
(41) van der Schaft, D. W.; Dings, R. P.; de Lussanet, Q. G.; van Eijk, L. I.; Nap, A. W.; Beets-Tan, R. G.; Bouma-Ter Steege, J. C.; Wagstaff, J.; Mayo, K. H.; Griffioen, A. W. The designer anti-angiogenic peptide anginex targets tumor endothelial cells and inhibits tumor growth in animal models. *FASEB J.* **2002**, *16*, 1991–1993.
(42) van Beijnum, J. R.; Nowak-Sliwinska, P.; van den Boezem, E.; Schulkens, I.; Hautvast, P.; Buurman, W.; Griffioen, A. Unpublished results: autocrine and paracrine regulation of HMGB1 enforces colon cancer progression through induction of angiogenesis.
(43) Lim, S. H.; Thivierge, C.; Nowak-Sliwinska, P.; Han, J.; van den Bergh, H.; Wagnieres, G.; Burgess, K.; Lee, H. B. In vitro and in vivo photocytotoxicity of boron dipyrromethene derivatives for photodynamic therapy. *J. Med. Chem.* **2010**, *53*, 2865–2874.